

1 **Simultaneous nitrification and denitrification using a novel up-flow**
2 **bio-electrochemical reactor**

3 Qi Tang^{1,2}, Meng Zheng¹, Yanqing Sheng^{1,*} and Robert J.G. Mortimer³

4 1 Research Center for Coastal Environment Engineering Technology of Shandong Province,
5 Yantai Institute of Coastal Zone Research, Chinese Academy of Sciences, Yantai 264003, China

6 2 University of Chinese Academy of Sciences, Beijing, China

7 3 School of Animal, Rural and Environmental Sciences, Nottingham Trent University,
8 Brackenhurst campus, Southwell, Nottinghamshire. NG25 0QF, UK

9 * Corresponding author; E-Mail: yqsheng@yic.ac.cn Tel.: +86-535-210-9265; Fax:
10 +86-535-210-9000.

11 Qi Tang, E-Mail: qtang@yic.ac.cn;

12 Meng Zheng, E-Mail: mzheng@yic.ac.cn;

13 Robert J.G. Mortimer, E-Mail: Robert.Mortimer@ntu.ac.uk

14 **Abstract:**

15 Nitrogen removal is a problem in the field of water treatment, especially in the
16 presence of sulfate. Conventional nitrification and denitrification are usually carried
17 out in two separate reactors. In addition, the effect of sulfate on hydrogenotrophic
18 denitrification is not clear. In this study, simultaneous nitrification and denitrification
19 (SND) for nitrogen removal from water was conducted using a single novel up-flow
20 bio-electrochemical reactor (UBER). The influence of dissolved oxygen (DO) on
21 nitrogen removal was investigated. When influent DO was 7.0 – 8.0 mg L⁻¹, a
22 heterotrophic nitrification zone (with DO 3.2 – 5.5 mg L⁻¹) and a hydrogenotrophic
23 denitrification zone (with DO 1.6 – 4.2 mg L⁻¹) were obtained within the reactor, and
24 the removal rates of NH₄⁺-N and TN reached more than 90%. The distribution of DO

25 inside developing biofilms was measured using microelectrodes. When DO in the
26 hydrogenotrophic denitrification zone was 2.9 mg L^{-1} , DO inside the biofilm was just
27 0.5 mg L^{-1} . The effect of sulfate on hydrogenotrophic denitrification was studied by
28 regulating the S/N ratio of influent water. Simultaneous removal of nitrate and sulfate
29 can be achieved at low S/N, and the removal rates of nitrate and sulfate were $\sim 80\%$.
30 With increasing S/N ratio, sulfide produced by sulfate reduction inhibited both
31 denitrification and further sulfate reduction.

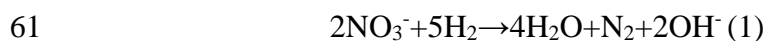
32 **Keywords:** Nitrification and denitrification; Bio-electrochemical reactor; Biofilm;
33 Sulfate

34 **1. Introduction**

35 Nitrogenous contaminants such as nitrate and ammonia can promote
36 eutrophication, causing deterioration of water quality and posing potential hazards to
37 human or animal health [1]. Therefore, different technologies such as reverse osmosis,
38 chemical denitrification and biological denitrification have been developed to remove
39 nitrogenous contaminants from water bodies [2]. Simultaneous nitrification and
40 denitrification (SND) is one of the most widely accepted biological solutions for
41 removing nitrogen from high ionic strength nitrogenous wastewaters [3]. SND is
42 highly effective at removing nitrogen compounds [4-5] because it uses small reaction
43 volumes, has short reaction times and low energy consumption [6-7]. It is estimated
44 that the SND process utilizes 22-40% less carbon and reduces sludge yield by 30%

45 compared with conventional nitrification and denitrification systems [8]. Through the
46 SND process, oxygen and NO_3^- -N can fully be utilized as the alternate electron
47 acceptors, which results in low DO [9-10]. Additionally, SND can be accomplished at
48 neutral pH because it is self-buffering, with alkalinity produced during denitrification
49 consumed during nitrification. Robertson *et al.* [11] reported that the experimental
50 conditions for SND were difficult to control in one reactor. Consequently, it is
51 necessary to develop a novel reactor for SND to ensure different microbial
52 communities are distributed effectively, and don't change with changing influent load.

53 The “bio-electrochemical reactor” system is a novel method for water and
54 wastewater denitrification that improves biological denitrification by immobilizing
55 autohydrogenotrophic bacteria directly on the surface of a cathode to provide easy
56 access to NO_3^- and H_2 as the electron acceptor and electron donor respectively [12].
57 Eq. (1) shows the general reaction leading to autohydrogenotrophic denitrification in
58 aqueous solution. Ghafari *et al.* [13] demonstrated co-existence of both aerobic and
59 anoxic zones in a single up-flow bio-electrochemical reactor (UBER), which had a
60 high chemical oxygen demand (COD) and efficient nitrogen removal.



62 Another limiting factor on N removal treatment systems is sulfate, which is
63 common in natural water bodies and wastewaters. Under anaerobic or anoxic
64 conditions, nitrate and sulfate can be reduced to nitrogen and sulfide by denitrifying
65 bacteria and sulfate reducing bacteria, respectively. Nitrate reduction is

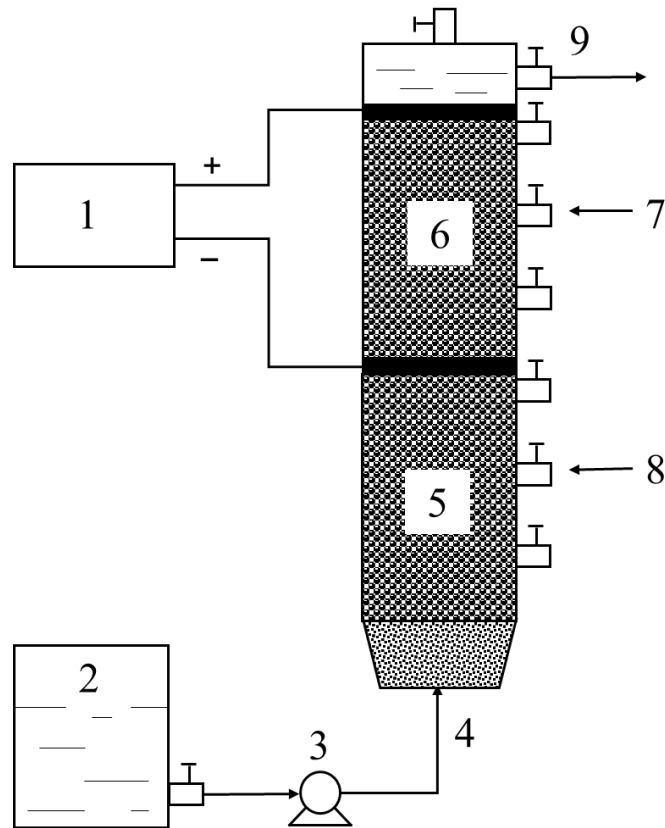
66 thermodynamically more favourable than sulfate reduction [14]. Chen *et al.* [15]
67 found that the degree of SO_4^{2-} reduction steadily decreased with higher influent NO_3^-
68 concentration. Conversely, the end product of sulfate reduction, sulfide, is harmful to
69 microorganisms at high concentration and has the potential to both inhibit N removal
70 processes and prevent further sulfate reduction. The relationship between nitrate and
71 sulfate in low DO environments therefore needs further study.

72 The goal of this study was (1) to design a novel reactor which combined
73 heterotrophic nitrification and hydrogenotrophic denitrification for SND (2) to
74 investigate nitrogen removal efficiency and DO distribution in biofilms in the reactor
75 (3) to explore the effect of sulfate on hydrogenotrophic denitrification.

76 **2. Materials and methods**

77 **2.1. Experimental apparatus**

78 A schematic of the lab-scale novel UBER used in the study is shown in Fig. 1.
79 The new UBER for SND was divided into two functional units, a lower heterotrophic
80 nitrification zone and an upper hydrogenotrophic denitrification zone, to ensure
81 different microbial communities were distributed effectively. The apparatus for
82 experiments on the effect of sulfate has the same volume and arrangement of
83 experimental materials but without the heterotrophic nitrification zone.



84

85 Fig. 1 Schematic of UBER for SND. (1) DC power supply; (2) influent tank; (3)
 86 influent pump; (4) inlet; (5) heterotrophic nitrification zone; (6) hydrogenotrophic
 87 denitrification zone; (7) sampling tap 1; (8) sampling tap 2; (9) outlet

88 The UBER was built using a 2 L Plexiglass cylindrical column (inside diameter
 89 of 9.2 cm, height 35cm), sealed at the top. A stainless steel wire mesh was installed at
 90 the middle of the reactor as a cathode and a carbon rod (8.8 cm long) was installed at
 91 the top of the reactor as the anode. An adjustable power supply (APS3005D,
 92 Shenzhen, China) was applied to provide direct current. One inlet port was installed at
 93 the bottom of the cylindrical column, and one outlet port was installed 27 cm from the
 94 bottom, leaving a 3 cm head space. Sampling points were installed every 5 cm from
 95 the bottom. Sampling tap 1 and tap 2 were installed 25 cm and 10 cm from the bottom,

96 respectively. The reactor was filled with carbon granules (in size range of 1-2 cm)
97 which were washed with deionized water four times prior to use. To provide a sticky
98 surface for microorganisms on the carbon granules, they were saturated and boiled in
99 2% agar solution. The total volume of carbon granules was 1 L, accounting for 50%
100 of the reactor's capacity. The reactor was covered with aluminium foil to exclude light
101 and prevent algal growth.

102 **2.2. Synthetic influent and sludge**

103 Based on the water quality that is characteristic of local polluted rivers, reservoirs
104 and groundwater [16], synthetic wastewater for this work was prepared with a low
105 C/N ratio. The composition of synthetic wastewater for the SND experiments
106 comprised; glucose (0.6 g L^{-1}), NH_4Cl (0.23 g L^{-1}), KH_2PO_4 (0.013 g L^{-1}),
107 $\text{MgSO}_4 \cdot 7\text{H}_2\text{O}$ (0.02 g L^{-1}), $\text{CaCl}_2 \cdot 2\text{H}_2\text{O}$ (0.001 g L^{-1}), $\text{FeSO}_4 \cdot 7\text{H}_2\text{O}$ (0.001 g L^{-1}),
108 NaHCO_3 (0.252 g L^{-1}) and 1 ml trace solution. The components of the trace solution
109 were $\text{ZnSO}_4 \cdot 7\text{H}_2\text{O}$ (100 mg L^{-1}), $\text{MnCl}_2 \cdot 4\text{H}_2\text{O}$ (30 mg L^{-1}), H_3BO_3 (300 mg L^{-1}),
110 $\text{CoCl}_2 \cdot 6\text{H}_2\text{O}$ (200 mg L^{-1}), $\text{CuCl}_2 \cdot 2\text{H}_2\text{O}$ (10 mg L^{-1}), $\text{NiCl}_2 \cdot 2\text{H}_2\text{O}$ (10 mg L^{-1}),
111 $\text{Na}_2\text{MoO}_4 \cdot 2\text{H}_2\text{O}$ (30 mg L^{-1}) and Na_2SeO_3 (30 mg L^{-1}). Oxygen (O_2) was added from
112 a gas cylinder to adjust the DO of the influent on demand. Aerobic and anaerobic
113 sludge were obtained from a secondary sedimentation tank and an anaerobic digester
114 tank in the Xin'anhe Municipal Wastewater Treatment Plant in Yantai, China. Aerobic
115 and anaerobic sludge were aerated with oxygen and bubbled with nitrogen,
116 respectively, for 24 h. The two kinds of activated sludge were mixed in equal volumes

117 prior to pouring (1 L) into the reactor.

118 The simulated wastewater composition for the sulfate effect experiments
119 comprised: NaHCO_3 (0.252 g L^{-1}), $\text{MgSO}_4 \cdot 7\text{H}_2\text{O}$ (0.34 g L^{-1}), FeCl_3 (0.1 g L^{-1}),
120 KH_2PO_4 (0.027 g L^{-1}), CaCl_2 (0.3 g L^{-1}), 1 ml trace solution I and 1 ml trace solution
121 II. The components in trace solution I were: EDTA (5 g L^{-1}), FeSO_4 (5 g L^{-1}). The
122 components in trace solution II were: EDTA (15 g L^{-1}), H_3BO_3 (0.014 g L^{-1}),
123 $\text{MnCl}_2 \cdot 4\text{H}_2\text{O}$ (0.99 g L^{-1}), $\text{CuSO}_4 \cdot 5\text{H}_2\text{O}$ (0.25 g L^{-1}), $\text{CoCl}_2 \cdot 6\text{H}_2\text{O}$ (0.24 g L^{-1}),
124 $\text{ZnSO}_4 \cdot 7\text{H}_2\text{O}$ (0.43 g L^{-1}), $\text{NiCl}_2 \cdot 6\text{H}_2\text{O}$ (0.19 g L^{-1}), $\text{Na}_2\text{MoO}_4 \cdot 2\text{H}_2\text{O}$ (0.22 g L^{-1}) and
125 $\text{Na}_2\text{SeO}_3 \cdot 10\text{H}_2\text{O}$ (0.21 g L^{-1}). The concentrations of NaNO_3 and Na_2SO_4 were added
126 as required for the experiment. The simulated wastewater was purged with nitrogen
127 for 1 h to remove residual oxygen. Anaerobic sludge was bubbled with nitrogen for 24
128 h before pouring (1 L) into the reactor.

129 **2.3. Experimental conditions**

130 The removal rates of $\text{NH}_4^+\text{-N}$ and total nitrogen (TN) in the reactor were
131 investigated under different conditions. At the beginning of the experiment, the pH of
132 the synthetic wastewater was adjusted to 7.5 using NaHCO_3 . The temperature was
133 controlled at $30 \pm 2^\circ\text{C}$ to accelerate the reaction rate and shorten the experimental
134 period. The bio-electrochemical reactor was operated with a feed of 200 ml/h
135 synthetic wastewater (hydraulic retention time = 10 h). DO concentration in the bulk
136 solution inside the reactor was set by adjusting inflow at different phases. The
137 UBER experiment lasted 95 days and was divided into 4 phases: days 1-30, 31-50,

138 51-70 and 71-95 (Table 1). These phase divisions ensured that the biofilm had enough
 139 time to mature and stabilize. In phase 1, the influent DO was adjusted to 5 mg L⁻¹.
 140 Consequently, the influent DO was adjusted to 6 mg L⁻¹ in phase 2, 7 mg L⁻¹ in phase
 141 3, and to 8 mg L⁻¹ in phase 4 (Table 1).

142 The effect of sulfate on hydrogenotrophic denitrification performance in the
 143 reactor was studied by regulating the influent S/N. Three experiments were conducted
 144 with S/N ratios of 1:2 (SO₄²⁻-S: 25mg L⁻¹, NO₃⁻-N: 50mg L⁻¹), 1:1(SO₄²⁻-S: 50mg L⁻¹,
 145 NO₃⁻-N: 50mg L⁻¹) and 2:1 (SO₄²⁻-S: 50mg L⁻¹, NO₃⁻-N: 25mg L⁻¹) respectively. The
 146 experiments were carried out at 30 ± 2°C, 10 mA electric current and 6 hours of
 147 hydraulic retention time until the effluent parameters were stable.

148 Table 1 Detailed operating conditions

	Phase1	Phase 2	Phase 3	Phase 4
Operation period (day)	30	20	20	25
Hydraulic retention time (h)	10	10	10	10
Electric current (mA)	20	20	20	20
Influent DO (mg L ⁻¹)	5	6	7	8
T (°C)	30	30	30	30
Influent NH ₄ ⁺ -N (mg L ⁻¹)	60	60	60	60

149 2.4. Sampling and analysis

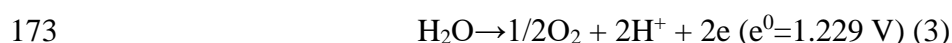
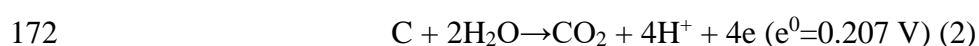
150 Samples were collected from the sampling taps. The pH, temperature (T) and DO
 151 were measured immediately using a pH meter (PSH-3C, China), thermometer, and
 152 oxygen microelectrode (PRO 3.0, Unisense, Denmark). The COD of the effluent was
 153 measured using the potassium dichromate method. Then, remaining water samples

154 were filtered using 0.2 μ m syringe filters prior to analysis for NH₄⁺-N, NO₃⁻-N, and
155 NO₂⁻-N using an Autoanalyzer III (Seal, Germany) with an analytical precision of
156 0.5‰ unit. SO₄²⁻-S and sulfide were analyzed by an ion chromatograph (Dionex
157 ICS3000, USA) and iodometric titration method [17] respectively. TN was detected
158 using an UV spectrophotometry meter (TU-1950, Persee, Beijing, China). The DO
159 distribution in the biofilm (adhered to the carbon granule surface) with depth was
160 measured using a miniaturized Clark-type oxygen sensor with a guard cathode (DO
161 microsensor, Unisense Microsensor, Denmark). A Micro Profiling System (Unisense)
162 was used to control the penetration distance and acquire data.

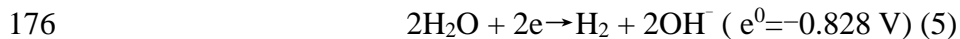
163 **3. Results and discussion**

164 **3.1. Start-up of the novel UBER**

165 DO level, electric current and hydraulic retention time are three important factors
166 in the nitrification and denitrification process. In this study, the novel UBER was
167 operated for 95 days (phases 1-4) with different influent DO values (Table 1). During
168 phase1, high current (20 mA), high temperature (30°C), short hydraulic retention time
169 (10 h) and 5.0 mg L⁻¹ DO were applied to supply sufficient substrates to support
170 microbial activity (inoculated aerobic sludge and anaerobic sludge). The possible
171 electrochemical reactions at the anode include:



174 And the possible electrochemical reactions at the cathode are



177 According to reaction (2) and (3), CO_2 is formed prior to O_2 at the anode. This CO_2
178 could serve as pH buffer and inorganic carbon source. The hydrogen gas produced
179 from the cathode serves as the electron donor for hydrogenotrophic denitrification.

180 Fig. 2 shows the variations in water quality between the lower and upper zone. In
181 the first two days, the effluent concentration of NH_4^+ -N was a little higher than initial
182 influent concentration (60 mg L^{-1}), which may be due to the death of bacteria which
183 cannot adapt to the influent conditions. In the lower zone, NH_4^+ -N and COD declined
184 sharply while NO_3^- -N increased gradually and remained stable during the whole
185 period. During phase 4, the steady concentrations of NH_4^+ -N, NO_2^- -N and NO_3^- -N
186 were 3.5 mg L^{-1} , 1.5 mg L^{-1} and 24.1 mg L^{-1} , respectively. There were $\sim 56.5 \text{ mg L}^{-1}$ N
187 removed as NH_4^+ -N and 25.6 mg L^{-1} N produced as NO_2^- -N and NO_3^- -N. The
188 removal rate of NH_4^+ -N reached 96.5% at the end of phase 4 (Fig. 2c). These results
189 indicate that nitrification occurred in the lower zone. This may include a variety of
190 nitrification reactions, such as heterotrophic nitrification and autotrophic nitrification.
191 In contrast chemoautotrophic nitrifiers, heterotrophic nitrifiers can use both inorganic
192 and organic substrates for nitrification [18-19]. A high C/N ratio can stimulate the
193 growth of heterotrophic bacteria and inhibit the activity of autotrophic nitrifiers [20].
194 In the presence of large amounts of organic matter, autotrophic nitrifying bacteria
195 have less competition for oxygen and organic matter than aerobic heterotrophic

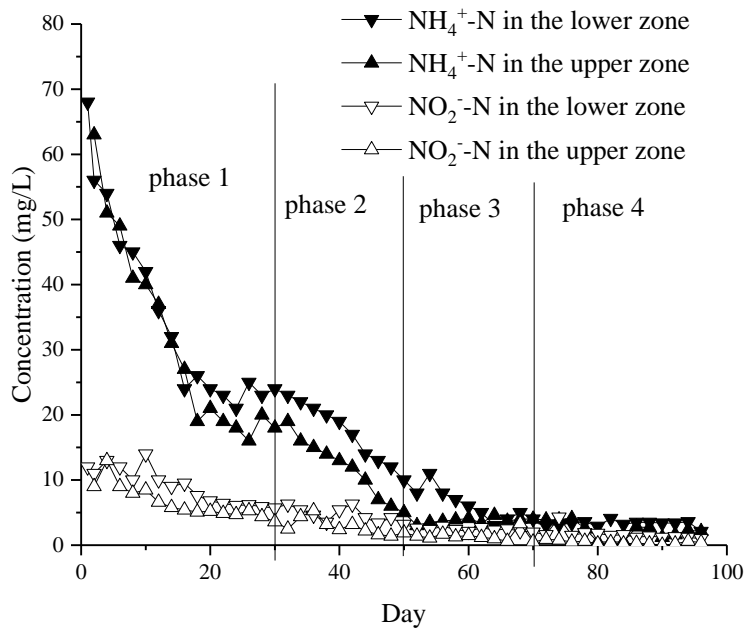
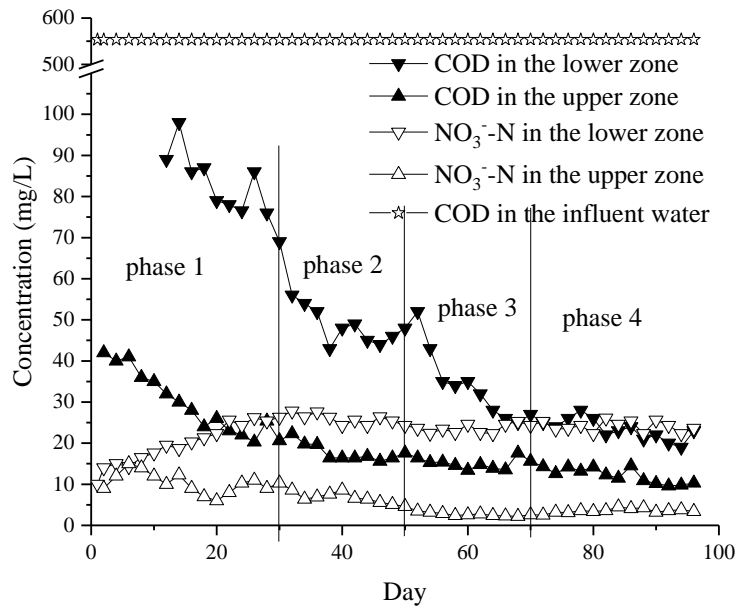
196 bacteria, allowing the heterotrophs to become predominant.

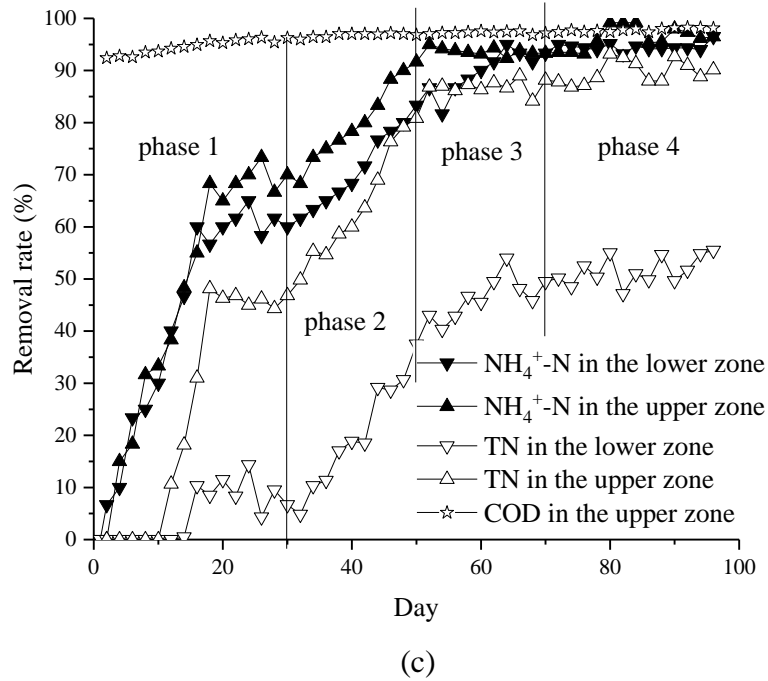
197 In the upper zone effluent water, there was no significant variations in $\text{NH}_4^+\text{-N}$
198 and $\text{NO}_2^-\text{-N}$ between the upper zone effluent and the lower zone effluent, but the
199 concentration of $\text{NO}_3^-\text{-N}$ showed a distinct decline. This implied that denitrification
200 mainly occurred in the upper zone. Both H_2 and organic matter can be used as
201 electron donor for denitrification in the reactor. The maximum denitrification rate in
202 the upper zone was $0.055 \text{ kg NO}_3^-\text{-N}/(\text{m}^3 \text{ d})$, and it was close to the similar
203 bio-electrochemical denitrification reactor, indicating that hydrogenotrophic
204 denitrification dominated in the upper zone.

205 In general, the hydrogenotrophic denitrification occurs at lower rates than
206 heterotrophic denitrification owing to slower bacterial growth rates [2]. For example,
207 Hamlin *et al.* used four kinds of organics as carbon sources and the obtained
208 maximum daily denitrification rate was $0.67\text{--}0.68 \text{ kg NO}_3^-\text{-N}/(\text{m}^3 \text{ d})$, regardless of
209 the carbon source [21]. The average denitrification rate was $0.62 \text{ kg NO}_3^-\text{-N}/(\text{m}^3 \text{ d})$ in
210 the ethanol supported system [22]. Sunger and Bose [23] achieved a denitrification
211 rate of $0.027 \text{ kg NO}_3^-\text{-N}/(\text{m}^3 \text{ d})$ in a fixed-bed hydrogenotrophic denitrification
212 system. Park *et al.* [24] achieved a higher denitrification rate ($0.077\text{--}1.68 \text{ kg}$
213 $\text{NO}_3^-\text{-N}/(\text{m}^3 \text{ d})$) using a bio-electrochemical reactor.

214 After 30 days, concentrations of $\text{NH}_4^+\text{-N}$, $\text{NO}_3^-\text{-N}$, and COD in the upper zone
215 effluent reached 19.2 mg L^{-1} , 8.6 mg L^{-1} , and 22.3 mg L^{-1} , respectively (Fig. 2).
216 Generally, stable water quality of the outlet and the color of biofilm can be used as

217 indicators of the mature status of the biofilm. In this study, stable water quality and
218 dark brown biofilm on the carriers (carbon granules) showed that the microbiological
219 UBER systems had established after 30 days. In the lower zone, NO_3^- -N increased to
220 26.3 mg L^{-1} at the end of phase 1 and remained at similar levels from phase 2 to phase
221 4. Meanwhile, NH_4^+ -N decreased to $\sim 3 \text{ mg L}^{-1}$ from phase 2 to phase 4, and the
222 removal rate of COD reached 95.8% at the end of phase 4. In the upper zone, after
223 phase 2, both of NO_3^- -N and NO_2^- -N were $< 5 \text{ mg L}^{-1}$, and NH_4^+ -N and COD kept low
224 levels ($\sim 5 \text{ mg L}^{-1}$ and $\sim 15 \text{ mg L}^{-1}$, respectively). These results demonstrate that
225 heterotrophic nitrification and hydrogenotrophic denitrification was stable in the
226 lower and upper zone respectively. As shown in Fig. 2(c), microbes maintained the
227 ability to remove organic matter with more than 90% COD removal rate during the
228 process of inoculation and acclimation (phase1). In the last phase, the removal rate of
229 COD was up to 98%. The COD removal efficiency of the bio-electrochemical reactor
230 was excellent.



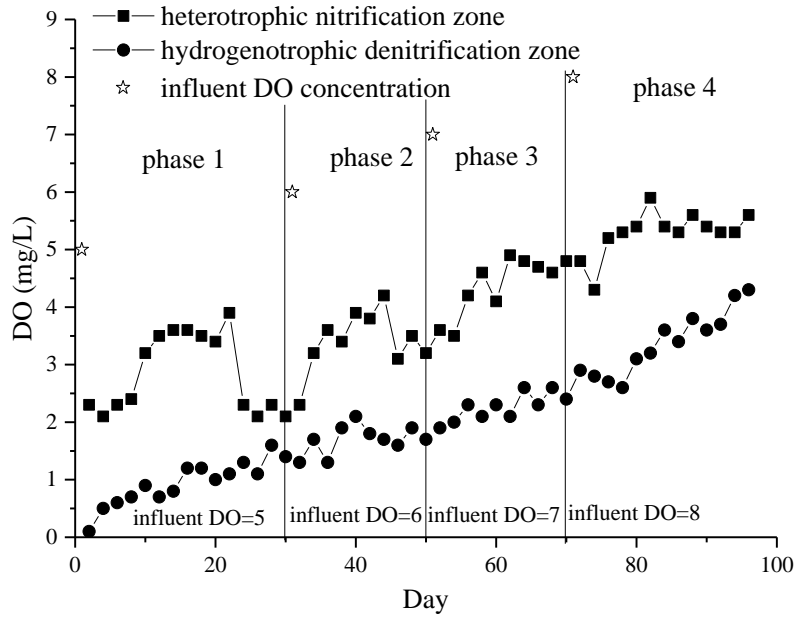


235
236

237 Fig. 2 Profiles of COD and NO_3^- -N (a), NH_4^+ -N and NO_2^- -N (b), and NH_4^+ -N and TN
238 removal rate (c) over time

239 **3.2. Influence of DO on the nitrogen removal**

240 During the experimental process, influent DO levels in influents were adjusted to
241 5, 6, 7 and 8 mg L^{-1} in phases 1, 2, 3 and 4, respectively. The relationship between DO
242 and nitrogen removal is shown in Fig. 2 and Fig. 3. As shown in the lower
243 heterotrophic nitrification section, the NH_4^+ -N and TN removal rates in phase 2 were
244 83.3% and 37.5%, respectively, with 3.2 mgL^{-1} DO. In phase 3, DO increased to 4.8
245 mg L^{-1} , and the removal rates of NH_4^+ -N and TN gradually increased to 93.3% and
246 49.5%, respectively (Fig. 2c). In the upper hydrogenotrophic denitrification section,
247 the removal rates of NH_4^+ -N and TN reached 80% while the DO level was 1.7 mg L^{-1}
248 at phase 2. In phase 3, NH_4^+ -N and TN removal rates achieved 90% with 2.4 mg L^{-1}
249 DO level (Fig. 2c).



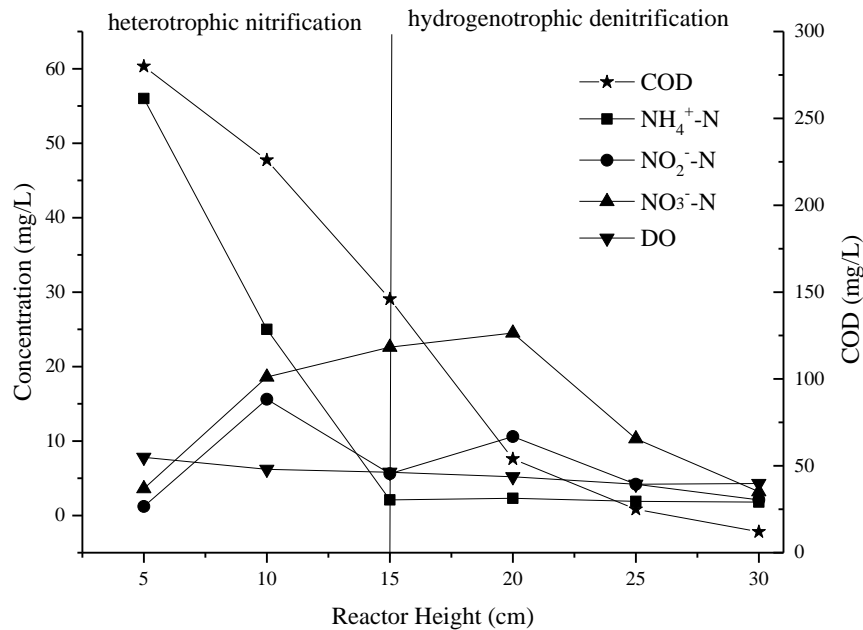
250

251 Fig. 3 Variations of DO in the heterotrophic nitrification zone and hydrogenotrophic
 252 denitrification zone

253 In phase 4, the DO levels in bulk solution increased further to 5.5 mg L⁻¹ and 4.2
 254 mg L⁻¹ in the heterotrophic nitrification and hydrogenotrophic denitrification zones,
 255 respectively, by increasing influent DO levels to 8.0 mg L⁻¹. At this stage, the effluent
 256 quality parameters such as NH₄⁺-N and NO₂⁻-N remained stable (Fig. 2). Meanwhile,
 257 the TN removal rates of the reactor were kept stable (above 90%). This phenomenon
 258 indicated that the hydrogenotrophic denitrification was not restricted by relatively
 259 high DO level (4.2 mg L⁻¹). Deng *et al.* [25] had similar results, showing that the
 260 autotrophic denitrification process using hydrogen from Fe–C galvanic cells as an
 261 electron donor was not affected by DO. Li *et al.* [26] also had similar findings, with
 262 maximum nitrogen removal efficiency of 96.5% while the DO concentrations of
 263 influent and effluent were 7.95 and 6.74 mg L⁻¹, respectively. As shown in Fig. 3, DO
 264 levels were well below the influent levels throughout. The decline of DO

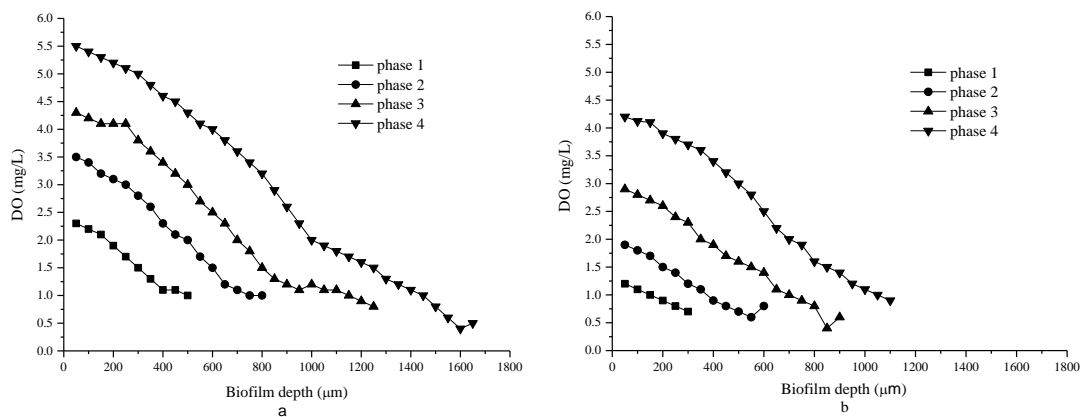
265 concentrations (about 1.3 mg L^{-1}) in the hydrogenotrophic denitrification zone
 266 between influent and effluent was likely due to consumption by aerobic denitrifiers
 267 [27]. The microbial community in the reactor needs to be studied.

268 **3.3. Simultaneous nitrification and denitrification**



269

270 Fig. 4 The water quality parameters at different depths of the reactor



271

272 Fig. 5 DO distribution in biofilms of the heterotrophic nitrification zone (left) and
 273 hydrogenotrophic denitrification zone (right) in four phases

274 At the end of the experiment (95 days, four phases), the concentrations of $\text{NH}_4^+\text{-N}$,
 275 $\text{NO}_3^-\text{-N}$, $\text{NO}_2^-\text{-N}$, TN and COD at different depths of the reactor were measured. As

276 show in Fig. 4, $\text{NH}_4^+\text{-N}$ and COD abruptly decreased to the lowest value (close to
277 zero) with depth. However, $\text{NO}_3^-\text{-N}$ increased gradually in the heterotrophic
278 nitrification zone (nitrification dominated the nitrogen removal process), then
279 decreased in the hydrogenotrophic denitrification section (denitrification dominated
280 the process); almost no $\text{NO}_2^-\text{-N}$ accumulated in the whole process. In the
281 heterotrophic nitrification zone, the concentration of $\text{NH}_4^+\text{-N}$ decreased from 56 mg
282 L^{-1} to 2.1 mg L^{-1} (Fig. 4) while both of $\text{NO}_3^-\text{-N}$ and $\text{NO}_2^-\text{-N}$ increased, which proved
283 that nitrification occurred. Meanwhile, the TN removal rate (above 50%) during phase
284 4 in Fig. 2c illustrates that significant denitrification took place in this point. As for
285 the hydrogenotrophic denitrification section, $\text{NH}_4^+\text{-N}$ and COD decreased gradually
286 with the reactor height, which showed partial nitrification could occur in this section.
287 $\text{NO}_2^-\text{-N}$ went up to 10.6 mg L^{-1} firstly and then reduced to 2.1 mg L^{-1} (Fig. 4),
288 moreover, there was similar variation trend in $\text{NO}_3^-\text{-N}$. This suggests both nitrification
289 and denitrification could occur in the upper denitrification zone. These phenomena
290 confirmed simultaneous nitrification and denitrification had been achieved in the
291 different parts of the reactor.

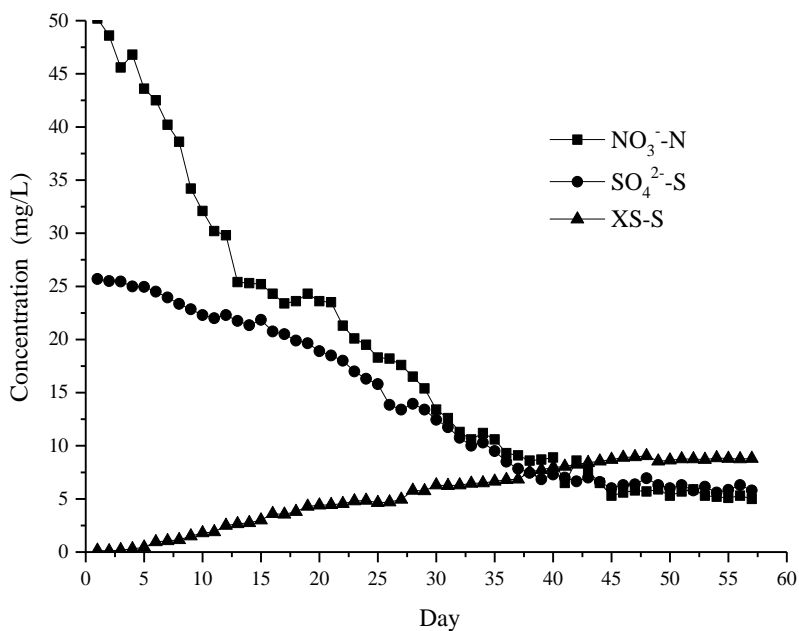
292 The transfer and consumption of DO in the biofilm serve important functions in
293 nitrogen removal in the UBER system. Excessively high DO transfer resistance in the
294 biofilm results in the aerobic layer being too thin and complicates ammonia oxidation.
295 Conversely, excessively low DO transfer resistance makes the anaerobic layer too thin
296 and slows down denitrification [28-29]. Determining the DO content in the biofilm is

297 helpful for understanding the mechanism of nitrogen removal. The DO
298 microdistributions (by microelectrode) in the nitrification and denitrification biofilms
299 are shown in Fig. 5. In the heterotrophic nitrification zone, the thickness of biofilm at
300 phase 1 was 500 μm and then increased with time. Consequently, the thickness of
301 biofilm increased to 1650 μm during phase 4. There was a similar pattern in the
302 hydrogenotrophic denitrification zone, where the thickest biofilm was 1100 μm at
303 phase 4. The thickness of both biofilms increased with time, showing a continued
304 growth of the microbial communities. It also can be seen that biofilm thicknesses in
305 the heterotrophic nitrification section were thicker than those in the hydrogenotrophic
306 denitrification section at the same phase. This result was in accordance with the fact
307 that heterotrophic microorganisms have faster growth rates than autotrophic
308 microbes. For the DO microdistribution in biofilms in the heterotrophic nitrification
309 zone (Fig. 5, left), the DO levels in the biofilm declined to approximately 1.1 mg L^{-1}
310 and then maintained a similar level, though the bulk DO values were different in
311 different phases. Similar trends were shown in the hydrogenotrophic denitrification
312 zone (Fig. 5, right), where the DO levels in the biofilms continuously dropped to
313 nearly 0.5 mg L^{-1} . The maximum DO in the upper and lower parts were 4.2 mg L^{-1}
314 and 5.5 mg L^{-1} , respectively. DO in biofilms decreased with the depth of biofilms at
315 all phases. Thus, nitrification occurred in the outer layer of the biofilms consumed
316 oxygen, which contributed to low DO conditions inside for anoxic denitrification. The
317 DO variation in the biofilms indicated that nitrification can occur in the outer layer of

318 the biofilms whereas denitrification can occur in the inner layer.

319 Overall, nitrification and denitrification for nitrogen removal with the UBER
320 system could be realized simultaneously. Simultaneous nitrification and denitrification
321 was not only achieved through the whole reactor but also in the individual
322 heterotrophic nitrification zone and hydrogenotrophic denitrification zone,
323 respectively.

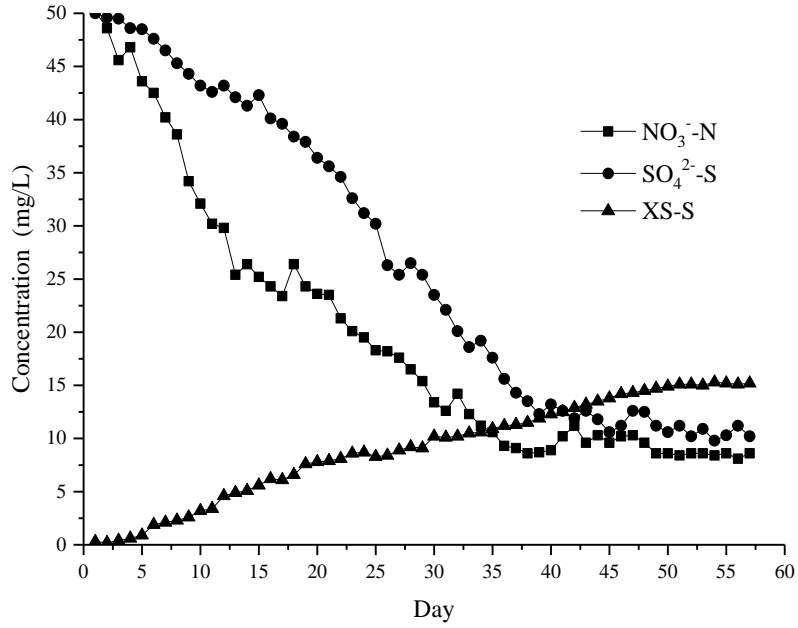
324 3.4. Effect of sulfate on hydrogenotrophic denitrification



325

326

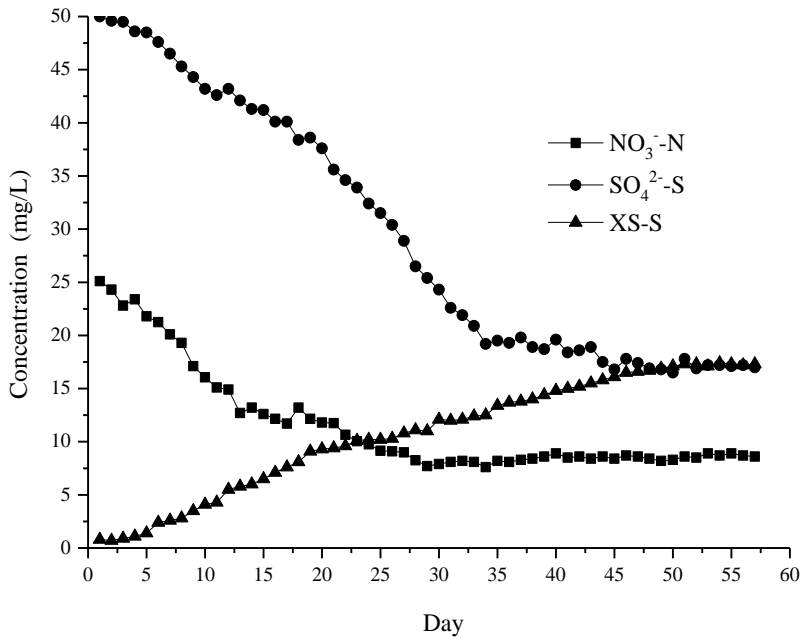
(a)



327

328

(b)



329

330

(c)

331 Fig. 6 The concentrations of substrate in the effluents of the reactor at different S/N

332 ratio (a)S/N=1:2; (b)S/N=1:1; (c)S/N=2:1 (XS-S refers to sulfide)

333 As shown in Fig. 6a, when the S/N ratio was 1:2, both effluent NO_3^- -N and

334 SO_4^{2-} -S decreased to $\sim 5 \text{ mg L}^{-1}$, the concentration of XS-S gradually increased to ~ 8

335 mg L⁻¹. The average removal rate of NO₃⁻-N (1 mg (L d)⁻¹) was significantly greater
336 than that of SO₄²⁻-S (0.44 mg (L d)⁻¹) when the effluent parameters remained stable.
337 The concentration of NO₃⁻-N and SO₄²⁻-S kept declining when the XS-S reached
338 about 8 mg L⁻¹. Finally, the removal rates of NO₃⁻-N and SO₄²⁻-S reached ~80%. The
339 results indicate that effective removal of nitrate and sulfate can be achieved
340 simultaneously at low S/N ratio since this concentration of XS-S (8 mg L⁻¹) didn't
341 inhibit hydrogenotrophic denitrification. Under a 1:1 S/N ratio, effluent SO₄²⁻-S
342 dropped to ~10 mg L⁻¹ and XS-S went up to 15 mg L⁻¹. When the effluent
343 concentration of NO₃⁻-N was higher than 15 mg L⁻¹(the first 13 days), the removal
344 rate of NO₃⁻-N (1.9 mg (L d)⁻¹) was greater than that of SO₄²⁻-S (0.54 mg (L d)⁻¹). The
345 effluent concentration of NO₃⁻-N remained stable (7 mg L⁻¹) after 37 days, while the
346 XS-S was 10 mg L⁻¹. At that stage, the average removal rate of SO₄²⁻-S was equal to
347 NO₃⁻-N (1.25 mg (L d)⁻¹). After 50 days, the XS-S increased to 15 mg L⁻¹ and the
348 SO₄²⁻-S reached a stable level (10 mg L⁻¹) (Fig. 6b). It can be inferred that the
349 denitrification process was inhibited when the XS-S reached 10 mg L⁻¹, and sulfate
350 reduction was inhibited when it reached 15 mg L⁻¹.

351 Results were similar with a S/N ratio of 2:1 (Fig. 6c). After 28 days, the
352 concentration of XS-S reached 10 mg L⁻¹ and effluent NO₃⁻-N was stable at about 7
353 mg L⁻¹. The average removal rate of NO₃⁻-N was similar to SO₄²⁻-S (0.7 mg (L d)⁻¹).
354 When the XS-S increased to 15 mg L⁻¹ at day 45, the SO₄²⁻-S equilibrium
355 concentration (15 mg L⁻¹) was achieved. Denitrification and sulfate reduction

356 processes were inhibited when the XS-S reached 10 mg L⁻¹ (day 28) and 15 mg L⁻¹
357 (day 45), respectively. The final removal rates of NO₃⁻-N and SO₄²⁻-S were below
358 68%. In the three groups of experiments, the denitrification percent declined and time
359 for stable effluent NO₃⁻-N shortened as S/N ratio increased. Further studies are
360 needed on how sulfate inhibits hydrogenotrophic denitrification: competition for
361 electronic donors or the toxicity of sulfide on denitrifying bacteria.

362 **4. Conclusions**

363 The SND could be achieved with the novel UBER system for synthetic
364 wastewater treatment. DO in bulk solution was an important factor that affected the
365 nitrification and denitrification processes in both heterotrophic nitrification and
366 hydrogenotrophic denitrification sections of the reactor. The experimental results
367 indicated that high nitrogen removal efficiency could be achieved through SND by the
368 UBER system. Relatively high DO concentration didn't inhibit hydrogen autotrophic
369 denitrification significantly. Simultaneous removal of NO₃⁻-N and SO₄²⁻-S can be
370 achieved at low S/N ratio, but higher ratios caused inhibition of denitrification and
371 sulfate reduction

372 **Acknowledgements**

373 This work was conducted with financial support from the Strategic Priority
374 Research Program of the Chinese Academy of Sciences (Grant No.:XDA23050203)
375 and the National Natural Science Foundation of China (Grant No: 41373100).

376 Additional supports were provided by the CAS Key Technology Talent Program.

377 **References**

- 378 [1] Y. Xiao, S. Wu, Z. H. Yang, Z. J. Wang, C. Z. Yan and F. Zhao, In situ probing the
379 effect of potentials on the microenvironment of heterotrophic denitrification
380 biofilm with microelectrodes, *Chemosphere.*, 93(2013), 1295-1300.
- 381 [2] F. Rezvani, M. H. Sarrafzadeh, S. Ebrahimi and H. M. Oh, Nitrate removal from
382 drinking water with a focus on biological methods: a review, *Environ. Sci. Pollut.*
383 *Res.*, 16(2017), 1-18.
- 384 [3] S. K. Gupta, S. M. Raja and A. B. Gupta, Simultaneous
385 nitrification-denitrification in a rotating biological contactor, *Environ. Technol.*,
386 15(1994), 145-153.
- 387 [4] S. B. He, G. Xue and B. Z. Wang, Factors affecting simultaneous nitrification and
388 denitrification (SND) and its kinetics model in membrane bioreactor, *J. Hazard.*
389 *Mater.*, 168(2009), 704-710.
- 390 [5] J. Guo, L. Zhang, W. Chen, F. Ma, H. Liu and Y. Tian, The regulation and control
391 strategies of a sequencing batch reactor for simultaneous nitrification and
392 denitrification at different temperatures, *Bioresour. Technol.*, 133(2013), 59-67.
- 393 [6] I. J. Kugelman, M. Spector, A. Harvilla and D. Paress, Aerobic denitrification in
394 activated-sludge, *Environ. Eng.*, 4(1991), 312-318.
- 395 [7] M. Morita, H. Uemoto and A. Watanabe, Nitrogen-removal bioreactor capable of
396 simultaneous nitrification and denitrification for application to industrial
397 wastewater treatment, *Biochem. Eng. J.*, 41(2008), 59-66.
- 398 [8] M. Seifi and M. H. Fazelipour, Modeling simultaneous nitrification and
399 denitrification (SND) in a fluidized bed biofilm reactor, *Appl. Math. Model.*,
400 36(2012), 5603-5613.
- 401 [9] X. Wang, S. Wang, J. Zhao, X. Dai and Y. Peng, Combining simultaneous
402 nitrification-endogenous denitrification and phosphorus removal with
403 post-denitrification for low carbon/nitrogen wastewater treatment, *Bioresour.*
404 *Technol.*, 220(2016), 17-25.
- 405 [10] L. Yan, S. Zhang, G. Hao, X. Zhang, Y. Ren, Y. Wen, Y. Guo and Y. Zhang,
406 Simultaneous nitrification and denitrification by EPSs in aerobic granular sludge
407 enhanced nitrogen removal of ammonium-nitrogen-rich wastewater, *Bioresour.*
408 *Technol.*, 202(2016), 101-106.
- 409 [11] L. A. Robertson, R. Cornelisse, V. P. De, R. Hadjoetomo and J. G. Kuenen,
410 Aerobic denitrification in various heterotrophic nitrifiers, *Antonie Van*
411 *Leeuwenhoek.*, 56(1989), 289-299.
- 412 [12] Y. Sakakibara and M. Kuroda, Electric prompting and control of denitrification,
413 *Biotechnol. Bioeng.*, 42(1993), 535-537.
- 414 [13] S. Ghafari, M. Hasan and M. K. Aroua, Nitrate remediation in a novel up flow
415 bio-electrochemical reactor (UBER) using palm shell activated carbon as cathode

- 416 material, *Electrochim. Acta.*, 54(2009), 4164-4171.
- 417 [14]A. Chidthaisong and R. Conrad, Turnover of glucose and acetate coupled to
418 reduction of nitrate, ferric iron and sulfate and to methanogenesis in anoxic rice
419 field soil, *FEMS Microbiol. Ecol.*, 31(2000), 73–86.
- 420 [15]C. Chen, X. J. Xu, P. Xie, Y. Yuan, X. Zhou, A. J. Wang, D. J. Lee and N. Q. Ren,
421 Pyrosequencing reveals microbial community dynamics in integrated
422 simultaneous desulfurization and denitrification process at different influent
423 nitrate concentrations, *Chemosphere.*, 171(2016), 294.
- 424 [16]M. Zheng, Y. Q. Sheng, R. C. Sun, C. G. Tian, H. B. Zhang, J. C. Ning, Q. R. Sun,
425 Z. R. Li, S. H. Bottrell and R. G. Mortimer, Identification and quantification of
426 nitrogen in a reservoir, Jiaodong Peninsula, China, *Water Environ. Res.*, 89(2017),
427 369-377.
- 428 [17]American Public Health Association/American Water Works Association/Water
429 Environment Federation, *Standard Methods for the Examination of Water and*
430 *Wastewater 20th edn*, Washington DC, USA,1998.
- 431 [18]W. De Boer and G. A. Kowalchuk, Nitrification in acid soils: micro-organisms
432 and mechanisms, *Soil Biol. Biochem.*, 33(2001), 853-866.
- 433 [19]J. Zhang, W. Sun, W. Zhong and Z. Cai, The substrate is an important factor in
434 controlling the significance of heterotrophic nitrification in acidic forest soils,
435 *Soil Biol. Biochem.*, 76(2014), 143-148.
- 436 [20]A. E. Amoo and O. O. Babalola, Ammonia-oxidizing microorganisms: key
437 players in the promotion of plant growth, *J. Soil Sci. Plant Nutr.*, 17(2017),
438 935-947.
- 439 [21]H. J. Hamlin, J. T. Michaels, C. M. Beaulaton, W. F. Grahama, W. Dutta P.
440 Steinbachb, T. M. Losordoc, K. K. Schraderd and K. L. Maina, Comparing
441 denitrification rates and carbon sources in commercial scale upflow
442 denitrification biological filters in aquaculture, *Aquacultural Engineering*,
443 38(2008), 79-92.
- 444 [22]Z. Q. Shen, Y. X. Zhou and J. L. Wang, Comparison of denitrification
445 performance and microbial diversity using starch/polylactic acid blends and
446 ethanol as electron donor for nitrate removal, *Bioresour. Technol.*, 131(2013),
447 33-39.
- 448 [23]N. Sunger and P. Bose, Autotrophic denitrification using hydrogen generated
449 from metallic iron corrosion, *Bioresour. Technol.*, 100(2009), 4077-82.
- 450 [24]H. I. Park, S. K. Ji, K. K. Dong, Y. J. Choi and D. Pak, Nitrate-reducing bacterial
451 community in a biofilm-electrode reactor, *Enzyme Microb. Technol.*, 39(2006),
452 453-458.
- 453 [25]S. H. Deng, D. S. Li, X. Yang, S. B. Zhu and J. L. Li, Process of nitrogen
454 transformation and microbial community structure in the Fe(0)-carbon-based
455 bio-carrier filled in biological aerated filter, *Environ. Sci. Pollut. Res.*, 23(2016),
456 6621-6630.
- 457 [26]P. Li, W. Xing, J. N. Zuo, L. Tang, Y. J. Wang and J. Lin, Hydrogenotrophic

- 458 denitrification for tertiary nitrogen removal from municipal wastewater using
459 membrane diffusion packed-bed bioreactor, *Bioresour. Technol.*, 144(2013),
460 452-459.
- 461 [27] J. C. Alzate Marin, A. H. Caravelli and N. E. Zaritzky, Nitrification and aerobic
462 denitrification in anoxic-aerobic sequencing batch reactor, *Bioresour. Technol.*,
463 200(2015), 380-387.
- 464 [28] Y. F. Ning, Y. P. Chen, Y. Shen, N. Zeng, S. Y. Liu, J. S. Guo and F. Fang, A new
465 approach for estimating aerobic-anaerobic biofilm structure in wastewater
466 treatment via dissolved oxygen microdistribution, *Chem. Eng. J.*, 255(2014),
467 171-177.
- 468 [29] X. Wen, J. Zhou, J. L. Wang, X. X. Qing and Q. He, Effects of dissolved oxygen
469 on microbial community of single-stage autotrophic nitrogen removal system
470 treating simulating mature landfill leachate, *Bioresour. Technol.*, 218(2016),
471 962-968.